

# Wear in metal/silicon nitride sliding pairs

G. Akdogan<sup>a,1</sup>, T.A. Stolarski<sup>b,\*</sup>

<sup>a</sup>*School of Process and Materials Engineering, University of the Witwatersrand, Johannesburg, South Africa*

<sup>b</sup>*Department of Mechanical Engineering, Brunel University, Uxbridge, Middlesex UB8 3PH, UK*

Received 27 May 2002; received in revised form 15 July 2002; accepted 5 August 2002

## Abstract

Ball-on-rotating disc tests were conducted to assess the relative wear behaviour of various disc materials in contact with silicon nitride under lubricated environment at room temperature high load and high speed conditions. Some selected tests were also performed under unlubricated conditions for comparison. The discs were made of grey cast iron, Al-bronze, bronze, aluminium and stainless steel. The lubricant was commercial additive free mineral base oil having a viscosity grade of 68. The applied normal load ranged between 16 and 300 N. The sliding speed changed from 0.5 to 4.0 m/s. The behaviour of grey cast iron and Al-bronze in sliding contact with silicon was characterised by a decrease in wear with an increase in sliding speed. Bronze and aluminium experienced very high wear rates as sliding speed increased. Stainless steel exhibited high wear and also caused significant damage to silicon nitride. Severity of wear between stainless steel and silicon nitride increased with the speed. High wear occurred at both low and high sliding speeds, which were accompanied by high wear track temperatures on the disc surface. This phenomenon resulted in considerable wear on both mating surfaces.

© 2002 Elsevier Science Ltd and Techna S.r.l. All rights reserved.

**Keywords:** Wear; Metal/silicon nitride; Sliding pairs

## 1. Introduction

High hardness, high temperature properties, lightness, low thermal conductivity and high wear resistance make ceramics desirable in applications such as cylinder liners, turbo-charger parts, piston crowns, valve seats and guides, cam follower inserts where ceramics can perform without excessive wear.

High performance silicon nitride materials were developed for automotive engine wear parts, such as valves and cam followers, and proven effective. Key properties of silicon nitride are high strength over a wide temperature range, high fracture toughness, high hardness, outstanding wear resistance in both impingement and frictional environments, good thermal shock resistance, and good chemical resistance. Silicon nitride has been successfully used as rolling bearings in

machine tools, sliding bearings in water pumps [1] as well as components in vacuum and precision equipment. It has become attractive practice to adopt silicon nitride ceramics on cutting tools and high temperature applications because they retain good strength and high hardness up to 1200 °C [2]. Typical uses are rotating bearing balls and rollers, cutting tools, engine moving parts such as valves, turbocharger rotors, engine wear parts including cam followers, tappet shims, turbine blades, vanes, buckets, metal tube forming rolls and dies, precision shafts and axles in high wear environments. Silicon nitride based ceramics with higher thermal conductivity and improved wear resistance than conventional ceramics are considered to be extremely suitable for continuous cutting at high cutting speeds.

Until recently, however, research on the ceramics tribology has mainly been limited to ceramic–ceramic and ceramic–steel pairs in water environment. Sasaki [3] found a hydrated SiO<sub>2</sub> film formed on the worn surface when silicon nitride slid against silicon nitride in water.

Gates and Hsu [4] investigated the effect of a variety of chemical compounds in the lubrication of silicon nitride–silicon nitride pairs. They suggested that silicon

\* Corresponding author. Tel.: +44-1895-27400x2716; fax: +44-1895-256392.

E-mail address: mesttas@brunel.ac.uk (T.A. Stolarski).

<sup>1</sup> Presently Visiting Fellow at Department of Mechanical Engineering, Brunel University.

nitride surface reacted with hydroxyl groups of primary alcohols leading to strong lubrication effect.

Winn et al. [5] studied the friction and wear of silicon nitride and steel pairs in the presence of mineral oil containing anti-wear additive in a pin-on-disc machine at 100 °C. Their results indicated that  $\text{Si}_3\text{N}_4$  wear rates were as low as  $1 \times 10^{-11} \text{ mm}^3/\text{Nm}$ . They argued that silicon nitride wear was due to tribochemical polishing mechanism at sliding speeds between 0.06 and 1.0 m/s under 40 N load.

Zhou et al. [6] carried out sliding tests on  $\text{Si}_3\text{N}_4$ /steel pair with anti-wear additives under 117 N at speeds between 1.6 and 3.6 m/s. They said that zinc alkyl dithiophosphate (ZDDP) and tricresylphosphate (TCP) were successful in preventing the inter-diffusion and adhesion between rubbing surfaces.

Silicon nitride ceramics as cutting tool applications in machining cast iron and nickel-based alloys [7,8] were found to be successful. However, their performance for cutting steels was reportedly poor [9].

Skopp et al. [10] have stated that there was a pronounced wear reduction due to tribo-chemical protective layer formation observed at sliding velocities above 0.3 m/s at 1000 °C and at higher velocities above 1.0 m/s at 400 °C.

Melandri et al. [11] reported that the wear rate of  $\text{Si}_3\text{N}_4$  increased significantly at 900 °C during unlubricated sliding.

In unlubricated sliding contact of silicon nitride against steel, chemically accelerated abrasion was found to be dominant wear mechanism. The formation of ferrous deposits on silicon nitride and a protective layer on the steel resulting in greater wear of ceramics than of the metal was also observed [12].

Zhou et al. [13] investigated unlubricated wear behaviour of  $\text{Si}_3\text{N}_4$  in a ring-block tester at 30 N for 4 km. They concluded that silicon nitride decomposition was responsible for its wear although they failed to support this temperature dependent phenomenon.

Gao et al. [14] worked on  $\text{Si}_3\text{N}_4$ /white iron pair in the presence of distilled water. They observed that a tribo-film formed on the white iron which was believed protect both silicon nitride and white iron during sliding.

In the present work, wear behaviour of cast iron, stainless steel, aluminium, Al-bronze and a high-lead-tin bronze in sliding contact with silicon nitride at both reasonably high loads and sliding speeds was compared in both dry and lubricated conditions using ball-on-rotating disc configuration.

## 2. Experimental

All experiments were performed by using a ball-on-rotating disc tester where a stationary silicon nitride ball, which has a diameter of 12.7 mm is loaded against

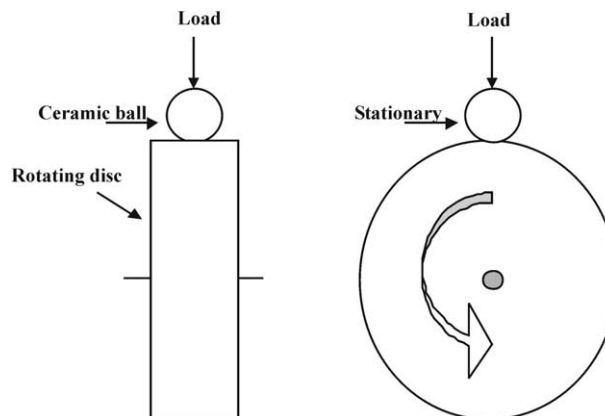


Fig. 1. Schematic representation of the experimental set-up.

the periphery of rotating counter face disc. The applied load was ranged from 16 to 300 N, which corresponds to contact pressures ranging from 0.8 to about 2 GPa. Fig. 1 depicts the schematic view of the experimental apparatus.

The spherical specimen was a hot isostatically pressed with 1% MgO sintering additive  $\text{Si}_3\text{N}_4$  ball bearing (NBD-200, Norton Advanced Ceramics). The density of the highly polished ball was  $3.16 \text{ g/cm}^3$ .

The rotating discs having a diameter of 120 mm were made of cast iron, Al-bronze, bronze, aluminium and stainless steel. Cast iron was pearlitic grey cast iron equivalent to BS1452 Grade 250. Al-bronze had Al 10%, Fe 5%, Ni 5% and Cu 80%. Bronze was SAE 660 high-lead-tin bronze containing Pb 7%, Sn 7% and Zn 3%. Aluminium disc was made from BS 6082 (H30) aluminium alloy. Stainless steel disc was made from alloy grade 316. The disc specimen surfaces were ground to a surface roughness of less than  $0.11 \mu\text{m}$ . The mechanical properties of discs and silicon nitride are given in Table 1.

The linear sliding velocity of the rotating discs was ranged from 0.5 to 4 m/s. Total sliding distance ranged from 1 to 5 km depending on the wear rate of the metal/silicon nitride pair type. In some instances the test was stopped due to sudden temperature increases along with very high level of noise. The contact was lubricated with an additive free base mineral oil namely Shell Vitrea 68 having a kinematic viscosity of 68 and 8.8 cSt at 40 and 100 °C respectively. A peristaltic

Table 1  
Some mechanical properties of disc and ball specimens

Material	Grey iron	Bronze 660	Al-bronze	St Steel 316	Al	$\text{Si}_3\text{N}_4$
Poisson ratio ( $\nu$ )	0.28	0.33	0.33	0.3	0.33	0.26
$E$ (GPa)	200	100	117	190	70	320

pump was used to pump the oil into the contact zone at a flow rate of 7 ml/min.

Prior to any test, surface roughness measurements and optical microscopy were conducted and initial inspection of the surface was carried out. Tests were interrupted at regular intervals to record the weight loss of the discs and ball specimens and to measure the temperature increase at the wear track by a K type thermocouple. Examination of the silicon nitride surface for wear scars and morphology was performed by using an optical microscope linked to video recorder and computer as well as by using a Cambridge Stereoscan 250 Mk2 SEM and JEOL JXA-840A microscope. Disc specimens were examined by the same manner under a light microscope. A Rank Taylor Hobson profilometer was used to inspect the changes taking place on the ball and disc surfaces at predetermined intervals. At each interval, eight measurements ( $R_a$ ) were made on different locations on the discs. Average value was taken as depth and width of the wear scars. The results of wear scar depth and width from were used to verify the weight loss measurements. From both weight loss and

wear scar dimensions wear volumes were calculated and the results agreed reasonably well. This procedure was carried out for silicon nitride ball as well.

All experiments were performed at ambient temperature of 21 °C and the relative humidity was about 35%. The load and speed were kept fixed during the duration of the test. Each type of disc was tested under the same conditions and results were reported according to wear scar width and diameter as well as with respect to specific wear rate. For every condition the test was repeated three times and the plotted wear data are the mean values recorded. A variation of about less than 10% in wear values was observed.

### 3. Results and discussion

The tests were carried out at 300 N for various sliding distances ranging from 1 to 5 km under lubricated conditions. Also some experiments were done on selected discs at 16, 122 and 300 N under both dry and lubricated conditions. All the tests were run for sliding

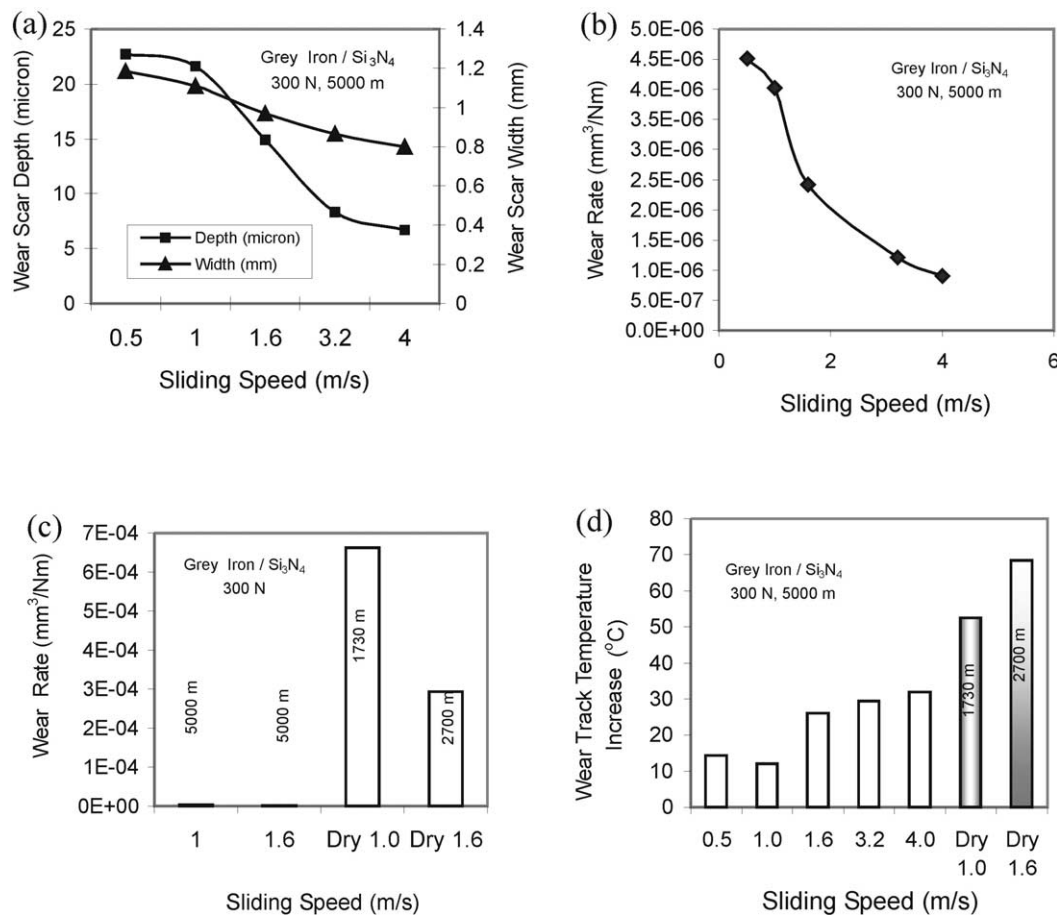


Fig. 2. Grey iron in sliding contact against Si<sub>3</sub>N<sub>4</sub>, (a) wear scar depth and width, (b) wear rate, (c) dry-lubricated wear rate, (d) increase in wear track temperature.

speeds ranging from 0.5 to 4.0 m/s. In the following section, wear scar dimensions of the discs and silicon nitride ball are given and wear rates of the discs are highlighted.

### 3.1. Grey cast iron–silicon nitride

Fig. 2(a) shows the change in wear scar dimensions of the grey cast iron disc against silicon nitride ball according to sliding speed at 300 N for a sliding distance of 5 km. As seen from the figure that as the sliding speed increased from 0.5 to 4.0 m/s depth and width of the wear scar on the disc decreased from about 22 to 7  $\mu\text{m}$  and from about 1.2 to 0.8 mm respectively. In Fig. 2(b) wear rate is given in terms of specific wear rate ( $\text{mm}^3/\text{Nm}$ ) and was calculated from surface profilometry and microscopic study which was also checked by using the weight loss measurements of the specimens. The wear rate of the disc decreased according to the speed as expected from wear scar dimensions from  $4.5 \times 10^{-6}$  to

$1 \times 10^{-6} \text{ mm}^3/\text{Nm}$ . Fig. 2(c) gives a comparison between lubricated and unlubricated (dry) sliding contact conditions at 1.0 and 1.6 m/s. During dry sliding wear rates were as much as  $6.5 \times 10^{-4} \text{ mm}^3/\text{Nm}$  although these tests were stopped at 1730 and 2700 m for 1.0 and 1.6 m/s due to very sharp increases in the temperature measured inside the wear track. The wear track temperature increase is the difference between instantaneous temperature in the wear track and initial temperature measured on the disc surface at the same point before the start of the test run. In Fig. 2(d) it is seen that the temperature increased during lubricated sliding as the sliding speed increased as expected except a slight decrease at 1.0 m/s. In the case of dry sliding, temperature increased very sharply after 1 km sliding distance. However, the wear rate of grey iron was found to be less at 1.6 than 1.0 m/s in both lubricated and unlubricated conditions, which might probably indicate that the wear mechanism of the grey cast iron is not significantly temperature dependent under the present experimental conditions.

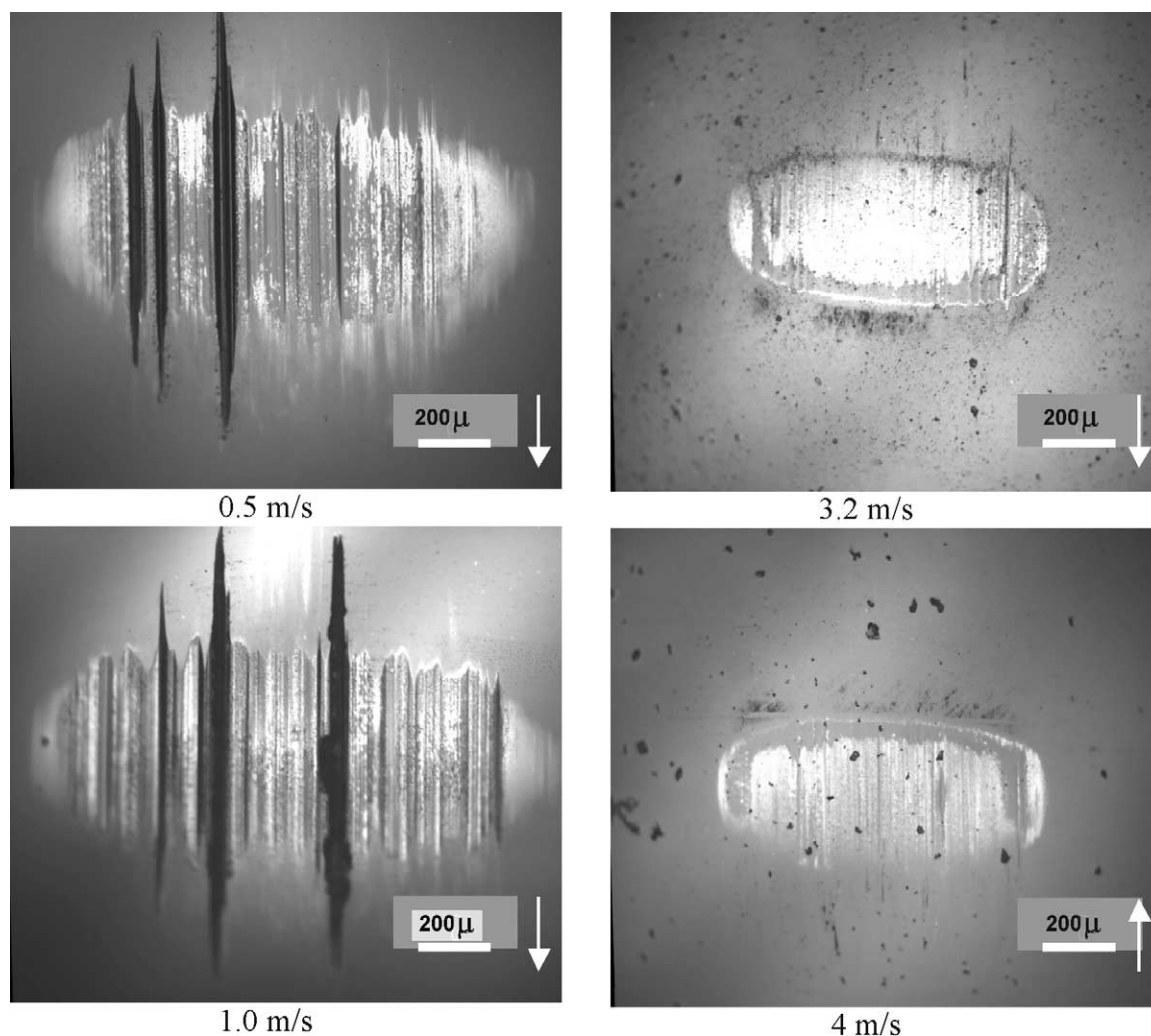


Fig. 3. Photomicrographs of wear scar on  $\text{Si}_3\text{N}_4$  surface against grey cast iron according to sliding speed.

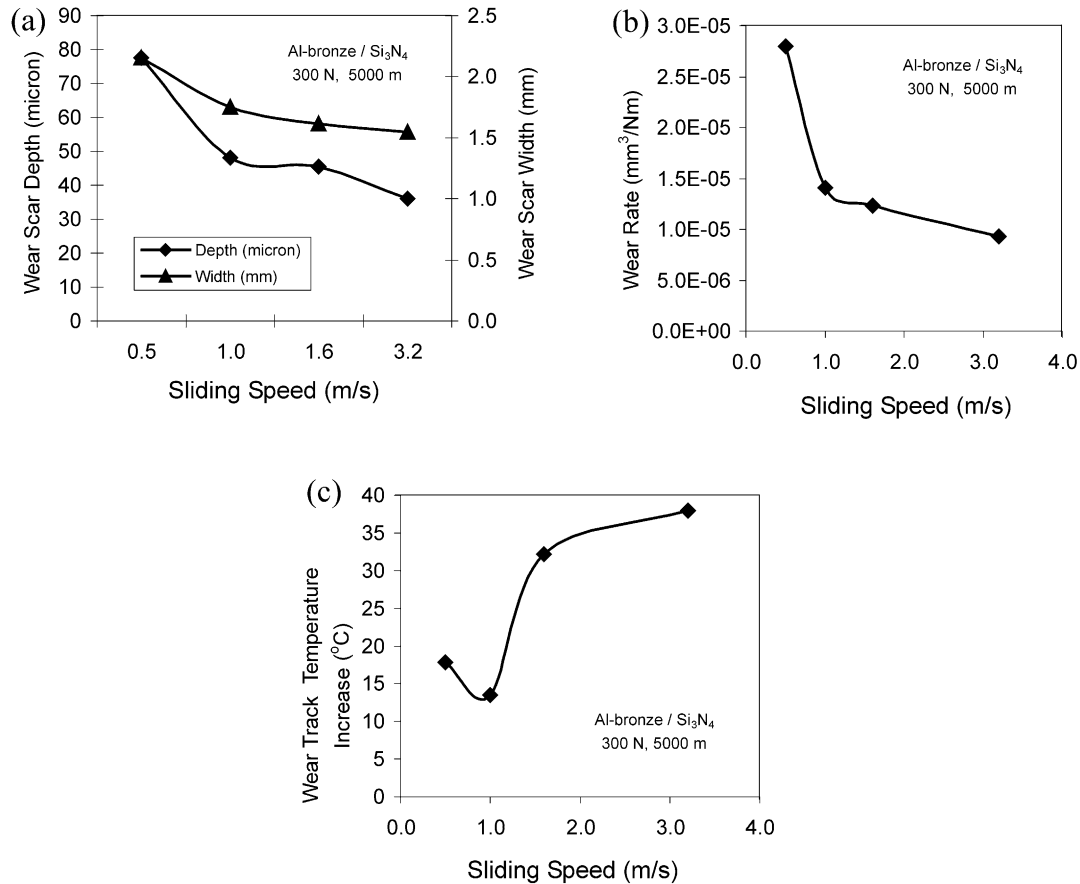


Fig. 4. Al-bronze in sliding contact against Si<sub>3</sub>N<sub>4</sub>, (a) wear scar depth and width, (b) wear rate, (c) increase in wear track temperature.

In Fig. 3 photomicrographs from optical microscope depict the effect of sliding speed on the wear scar dimensions of the silicon nitride ball at 300 N. As seen from the pictures, at low speeds wear scar surface was rough and contained several micro grooves filled with a metallic tribofilm. As the speed increased contact zone became smaller and smoother indicating an increase in effectiveness of the lubricating mineral based oil. Visual observations also showed a residue of the oil film on the edges of the contacts.

### 3.2. Al-bronze–silicon nitride

Fig. 4(a) shows the wear scar depth and width according to sliding speed. Similar to the grey cast iron behaviour, the wear scar depth and width decreased from 80 to about 35  $\mu\text{m}$  and from 2.2 to about 1.0 mm respectively as the sliding speed increased. The wear rate also decreased with the speed from about  $2.8 \times 10^{-5}$  to  $9 \times 10^{-6}$  mm<sup>3</sup>/Nm [Fig. 4(b)]. Fig. 4(c) gives the wear track temperature increase during the test relative to the initial value. After an initial decrease to 12 °C at 1.0 m/s from 18 °C at 0.5 m/s, it increased gradually to about 38 °C at 3.2 m/s.

Fig. 5 features wear scar photomicrographs on the silicon nitride ball specimen for varying speeds. It also shows that the wear scar became smoother as the speed increased. Although the elliptical contact width and depth were larger than that of the grey cast iron/silicon nitride pair, they were significantly smaller as compared to the other couples. Also it was notable that the dimensions of the contact became smaller with speed.

### 3.3. Bronze 660–silicon nitride

In contrast to grey cast iron and Al-bronze, the wear scar dimensions increased dramatically with the sliding speed during the course of the tests. Fig. 6(a) shows that scar depth increased from 120 to 180  $\mu\text{m}$  as the sliding speed increased from 0.5 to 1.6 m/s. Similarly, the scar width increased from 1.5 to 3.2 mm within the same speed range [Fig. 6(b)]. The wear rate also increased significantly with the sliding speed [Fig. 6(c)]. Fig. 6(d) displays that the wear track temperature increase became greater with the speed. However, at a sliding speed of 3.2 m/s wear track temperature increased tremendously and the temperature difference between initial and instantaneous value was about 45 °C. Also



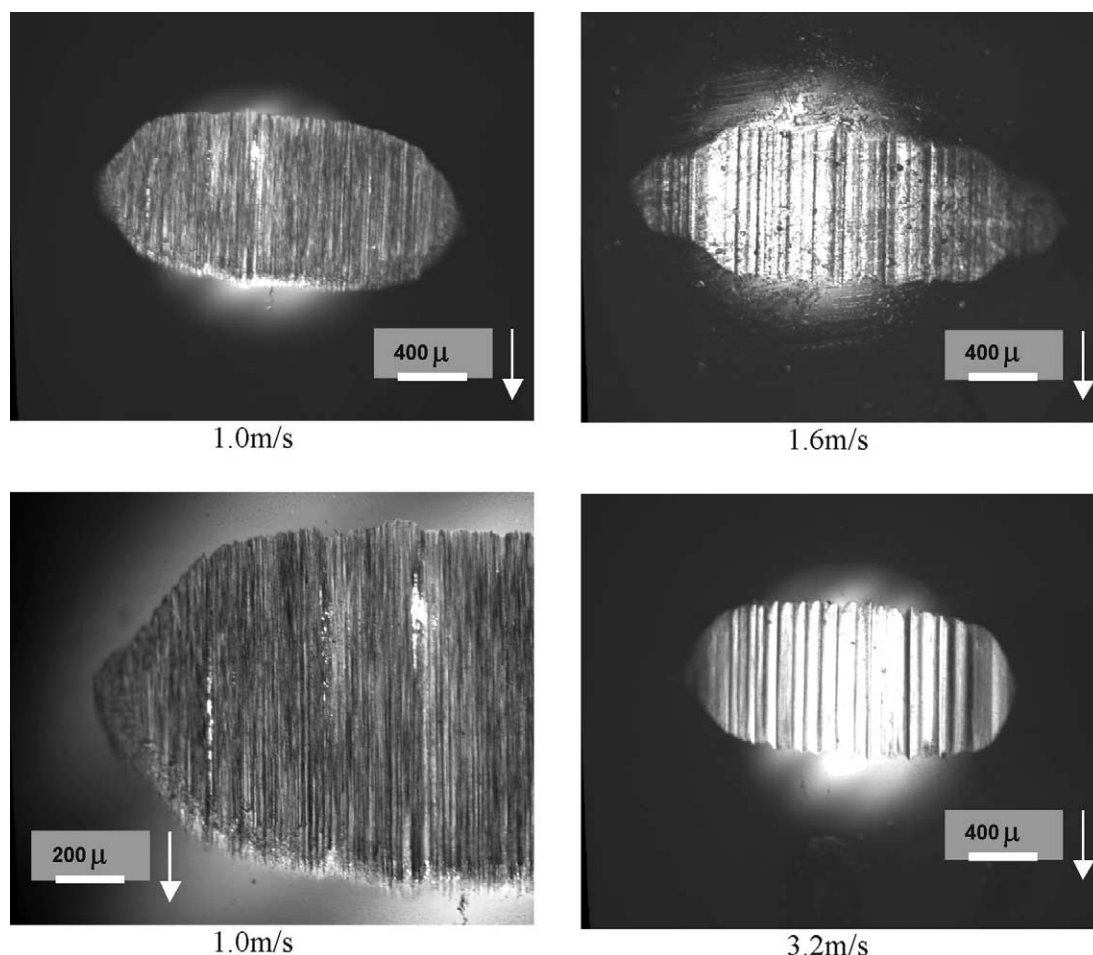


Fig. 5. Photomicrographs of wear scar on  $\text{Si}_3\text{N}_4$  surface against Al-bronze according to sliding speed.

the sliding contact became unbearably noisy and the test was stopped at 1730 m.

Fig. 7 gives details of contact zone on the silicon nitride ball with an increase in the sliding speed. As can be seen initially at 0.5 m/s the wear scar perpendicular to the sliding direction had a needle like shape formed by the metallic debris from the bronze disc. As the speed increased the width and the length of this metallic tribofilm increased.

### 3.4. Aluminium–silicon nitride

Fig. 8(a) displays the wear rate of the aluminium disc with respect to load applied. The wear rate increased with the sliding speed from  $3 \times 10^{-5}$  to about  $5.5 \times 10^{-5} \text{ mm}^3/\text{Nm}$  between 0.5 and 1.0 m/s respectively at 300 N. At a constant speed of 0.5 m/s, the wear rate was minimal when it was compared with 300 N. Also again at 0.5 m/s, the wear rate increased by almost 4 times with an increase in the normal load from 122 to 300 N. It was noticed that aluminium behaved very similar to the

bronze 660 in that wear rate increased with the sliding speed at a fixed load. Even the interface temperature increase was found to be almost in the same order with the bronze/silicon nitride system at 300 N [Fig. 8(b)]. It was also seen that the wear track temperature increase rose from about 7 to 17 °C with an increase in the load from 16 to 300 N at 0.5 m/s.

Photomicrographs in Fig. 9 also support the above findings that at 16 N loading the wear scar on the ball was hardly noticeable and looked very much like a slight scratch. At 122 N it became larger with an elliptical shadowy view. At 300 N and at 0.5 m/s sliding speed, there is considerable metallic debris accumulation on the outer boundary of the contact especially in the sliding direction.

### 3.5. Stainless steel–silicon nitride

Fig. 10(a,b) exhibits that depth and width of the wear scar decreased from 180 to about 50 μm and from 3 to 1.75 mm for sliding speeds from 0.5 to 1.0 m/s respectively.

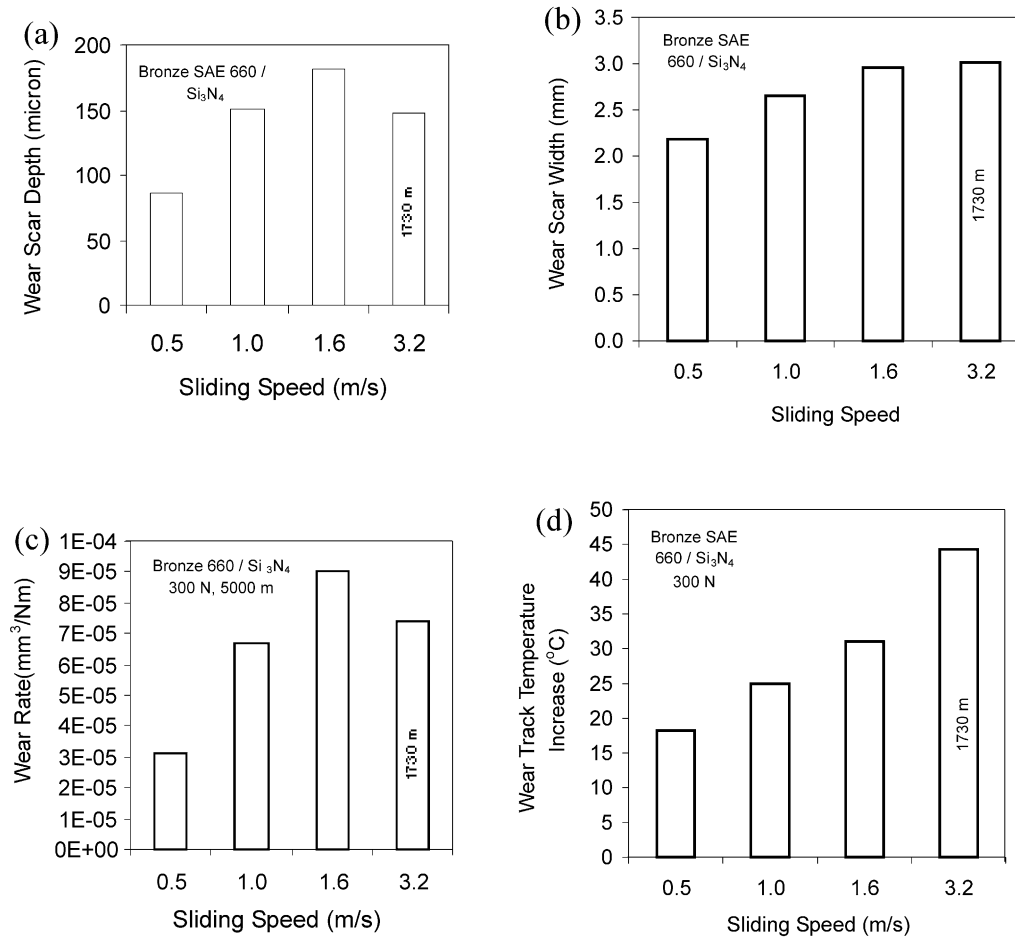


Fig. 6. Bronze 660 in sliding contact against Si<sub>3</sub>N<sub>4</sub>, (a) wear scar depth, (b) wear scar width, (c) wear rate, (d) increase in wear track temperature.

After that, the wear scar dimensions increased slightly to 80  $\mu\text{m}$  in depth and 2.2 mm in width. At 3.2 m/s, however, there was a considerable jump to very high values for even relatively short sliding distances. For instance, depth of the wear scar was about 190  $\mu\text{m}$  and the width was nearly 2.7 mm for a sliding distance of 1730 m. As expected from the wear scar dimensions, the wear rate also followed the same trend after 1.6 m/s sliding speed [Fig. 10(c)]. The wear rate was  $8.5 \times 10^{-5} \text{ mm}^3/\text{Nm}$  at a speed of 3.2 m/s for a sliding distance of 1730 m. The wear track temperature increase remained almost at a fixed value of about 25  $^{\circ}\text{C}$  at sliding speeds between 0.5 and 1.6 m/s [Fig. 10(d)]. At 3.2 m/s temperature increase was up sharply to about 65  $^{\circ}\text{C}$  at a sliding distance of 1730 m. During this period high levels of grinding-like noise and vibration were observed. As a result the tests were discontinued after this distance at 3.2 m/s sliding speed. At higher speeds situation was progressively worse and the tests were abandoned entirely.

Fig. 11 represents the effect of sliding speed on silicon nitride ball in contact with stainless steel. It also highlights

the severity of the silicon nitride wear at 300 N under lubricated conditions. It was noticeable that the formation of ring cracks on the ceramic surface was followed by failure within the boundary of the elliptical contact.

#### 4. Discussion

The experimental results indicated that the observed behaviour of the discs used during the sliding tests against silicon nitride under mineral oil lubrication at reasonably high loads and high speeds could be classified into three main groups:

The first group comprised of grey cast iron and Al-bronze. The tribological behaviour of this group was characterised by lowest wear rates at all sliding speeds and also by a decrease in wear with an increase in sliding speed. Another distinctive feature was modest temperature increase in the wear track as the sliding progresses. There was no metallic debris formation observed on the ceramic ball. Also visual observations showed that the damage on the ball surface was

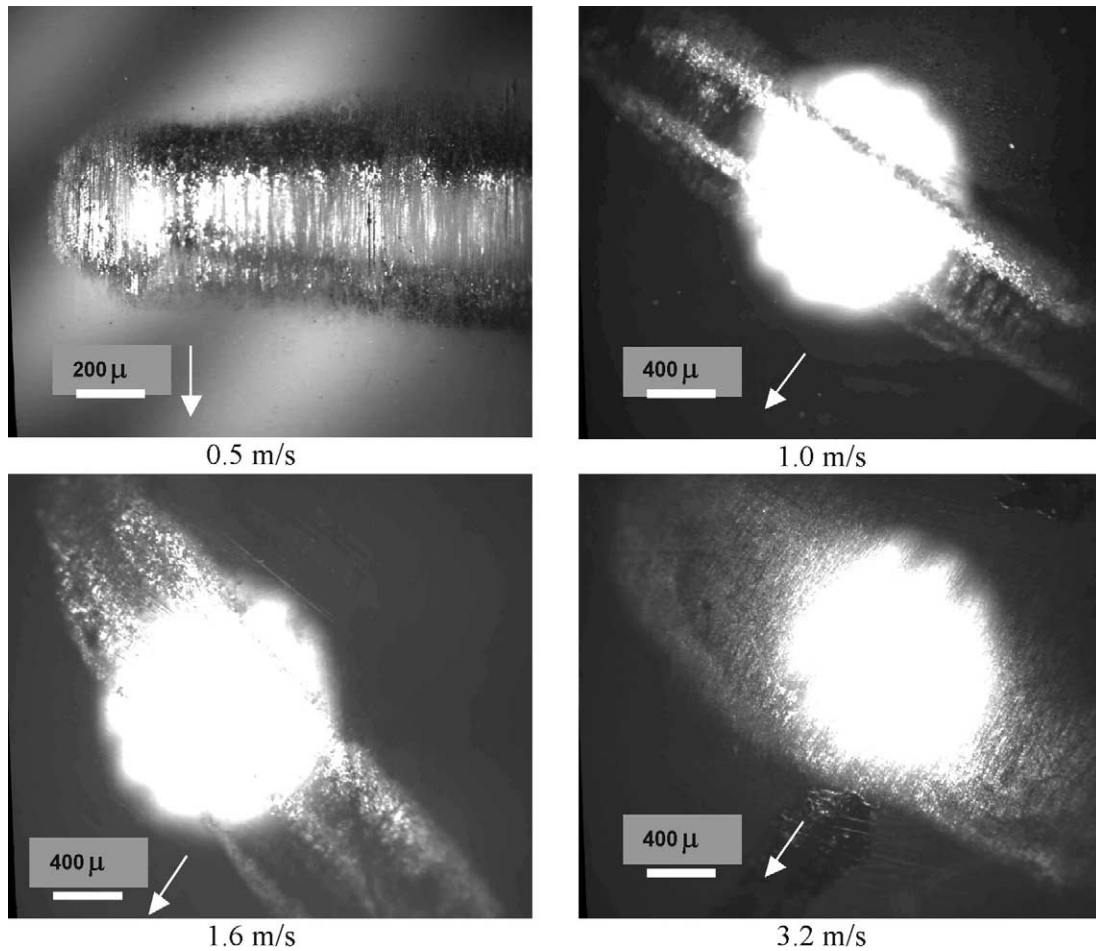


Fig. 7. Photomicrographs of wear scar on  $\text{Si}_3\text{N}_4$  surface against bronze 660 according to sliding speed.

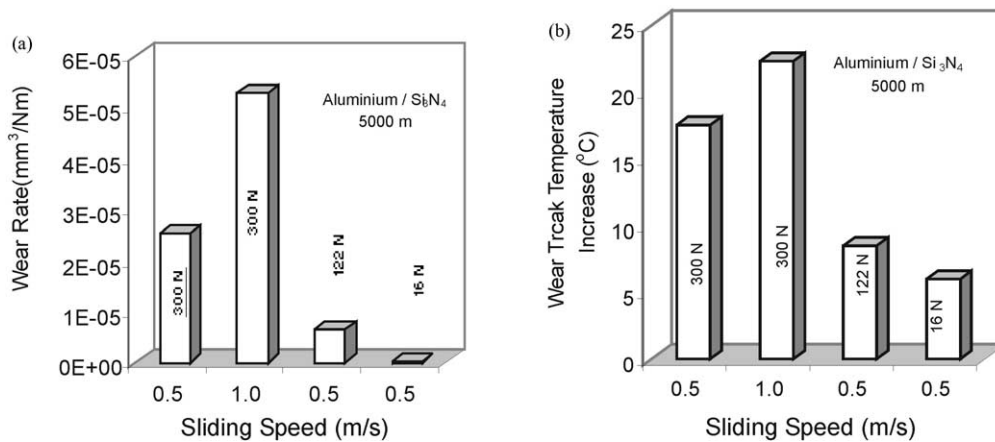


Fig. 8. Al-bronze in sliding contact against  $\text{Si}_3\text{N}_4$ , (a) wear rate, (b) increase in wear track temperature.

insignificant especially at high sliding speeds. Grey cast iron experienced very low wear rates during sliding contact with silicon nitride. The increase in the wear track temperature from an initial ambient temperature stayed relatively lower despite a gradual increase with

sliding speed reaching a maximum of  $30^{\circ}\text{C}$  at  $4.0\text{ m/s}$ . As the speed increased wear rate decreased. Microscopic examinations revealed that the worn surfaces became smoother and smaller at higher sliding speeds, which showed an increase in lubricant effectiveness. A metallic



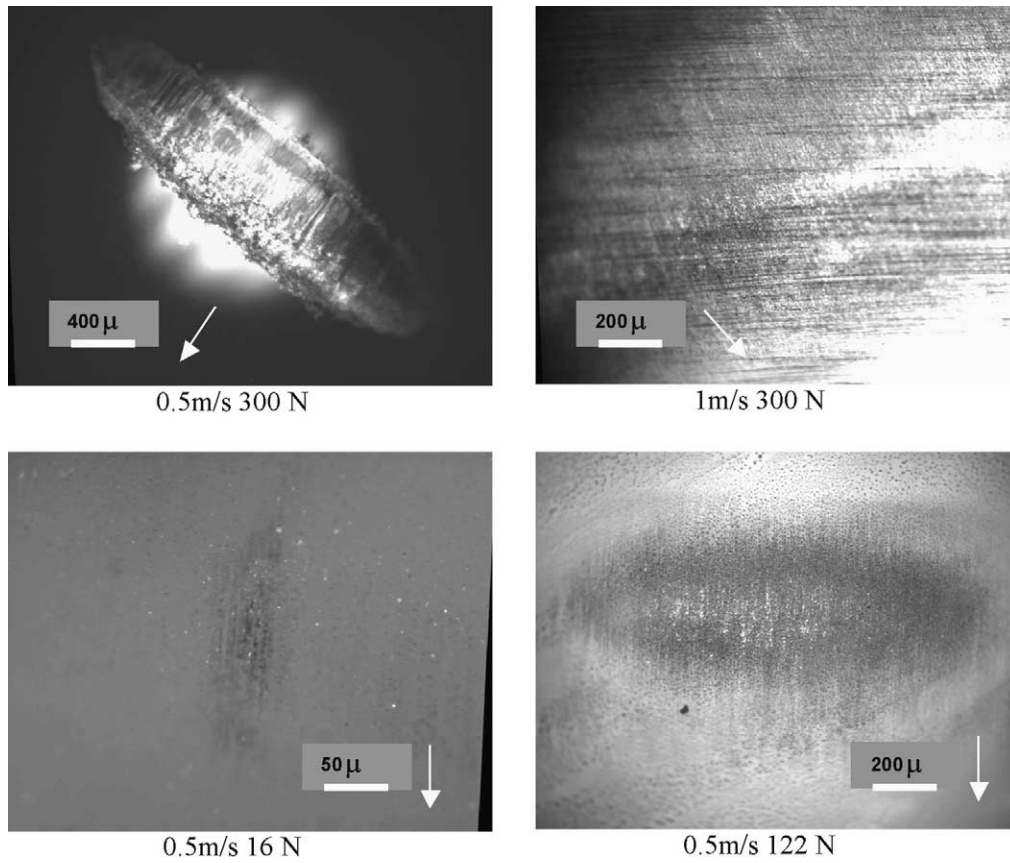


Fig. 9. Photomicrographs of wear scar on  $\text{Si}_3\text{N}_4$  surface against aluminium according to sliding speed.

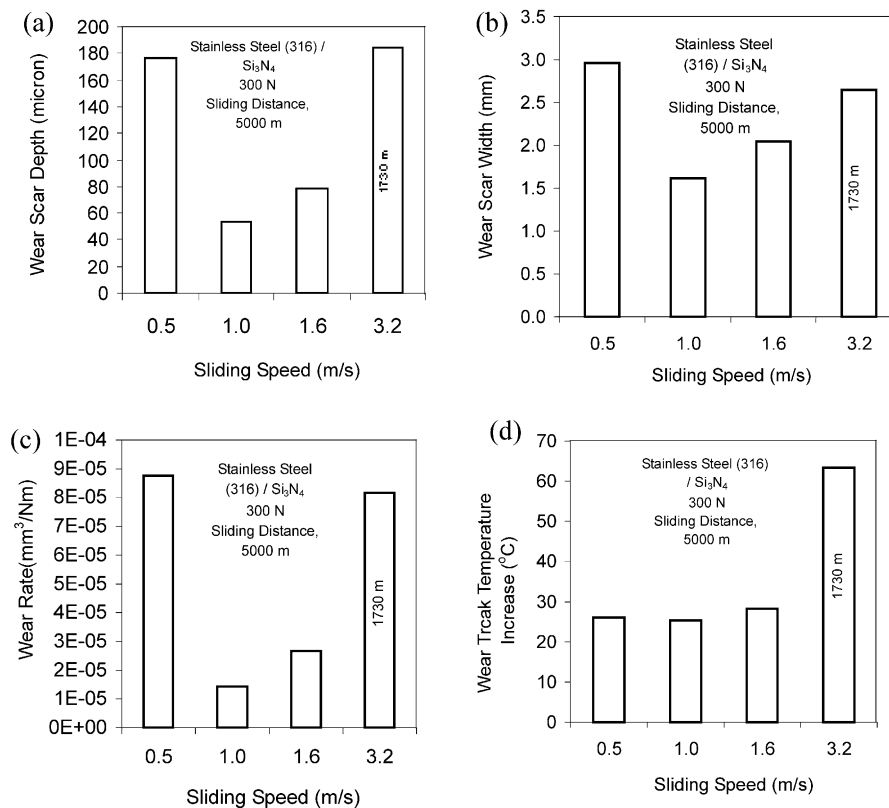


Fig. 10. Stainless steel in sliding contact against  $\text{Si}_3\text{N}_4$ , (a) wear scar depth, (b) wear scar width, (c) wear rate, (d) increase in wear track temperature.

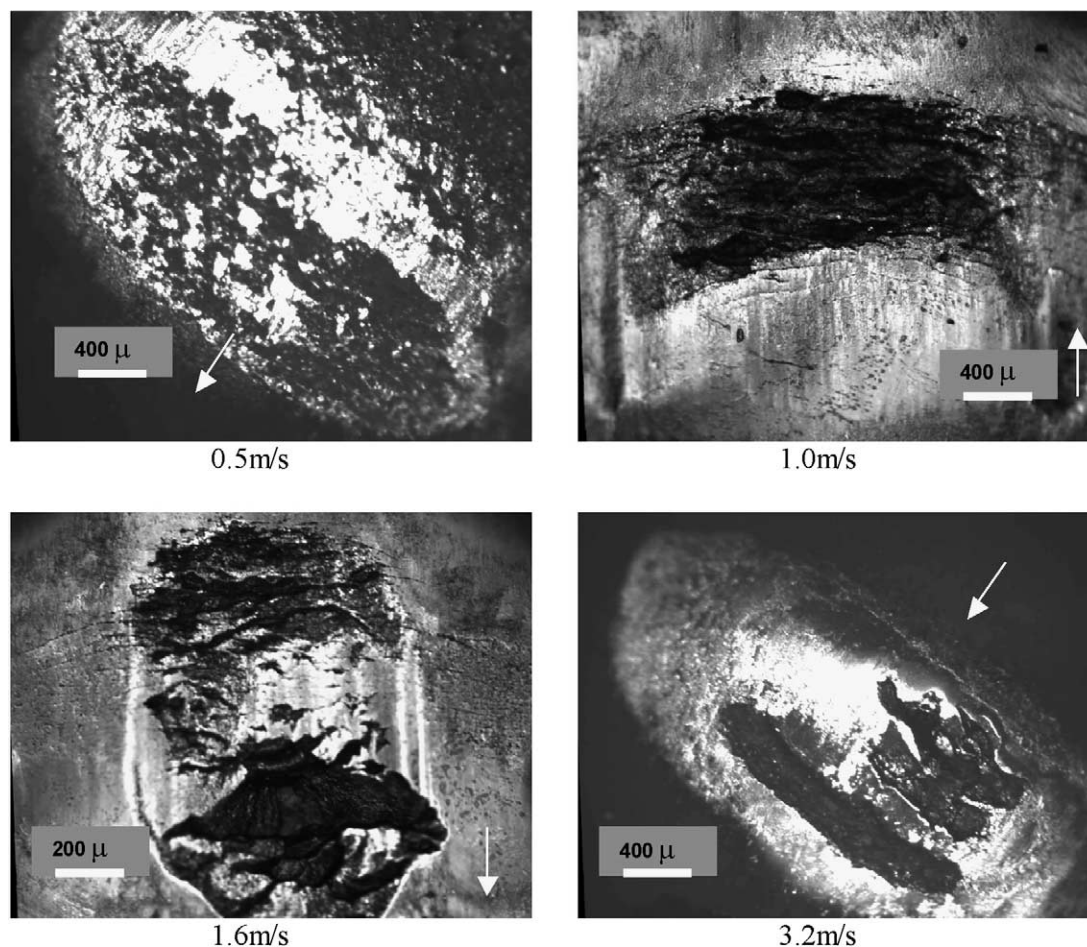


Fig. 11. Photomicrographs of wear scar on  $\text{Si}_3\text{N}_4$  surface against stainless steel according to sliding speed.

debris collected by filtering the lubricant contained particles having an average diameter of about 0.25 mm indicating that third body abrasion was operative especially at low speeds causing wider and deeper wear scars on both surfaces. Grey cast iron was undoubtedly the best sliding wear resistant material under the present experimental conditions. Al-bronze behaviour was found to be nearly similar to that of grey cast iron despite the fact that it had higher wear rates than those of grey iron at all speeds. Similar to the grey cast iron the sliding speed increase affected Al-bronze positively and the wear rates were lowered as the speed increased. Overall, it was found to be the second best material in sliding wear resistance.

The second group consisted of high-lead-tin bronze (bronze 660), aluminium. This groups distinguishing mark was very high wear rates as sliding speed increased. The rise in the wear track temperature became significantly steeper with speed. Overall, they exhibited extremely poor resistance to sliding as expected due to their low hardness features. A metallic tribofilm/debris formation was visible at even very low speeds and low loads. The debris included very fine

plate-like smooth particles sizing about less than 50  $\mu$ . This film was not easily detachable indicating some form of chemical interaction with the silicon nitride surface due to high interface temperature during sliding process. It was also noticed that the wear damage on the ceramic surface increased with the sliding speed.

The third group contained stainless steel, which displayed entirely different behaviour as compared to the other materials. During stainless steel–silicon nitride sliding contact microfracture took place in the contact zone. A metallic tribofilm was seen on the ceramic ball surface even at low speeds. Severity of wear between stainless steel and silicon nitride increased with the speed. Very high wear track temperatures and unbearable noise levels always accompanied high wear rates. Worn surfaces looked very rough and considerable wear occurred on both surfaces. The debris collected by filtering the lubricant contained metallic particles as large as 0.3 mm indicating that third body abrasion might be possibly responsible for high level of wear on both surfaces.

Overall wear behaviour of the materials are summarised according to sliding speed in Fig. 12. As can be

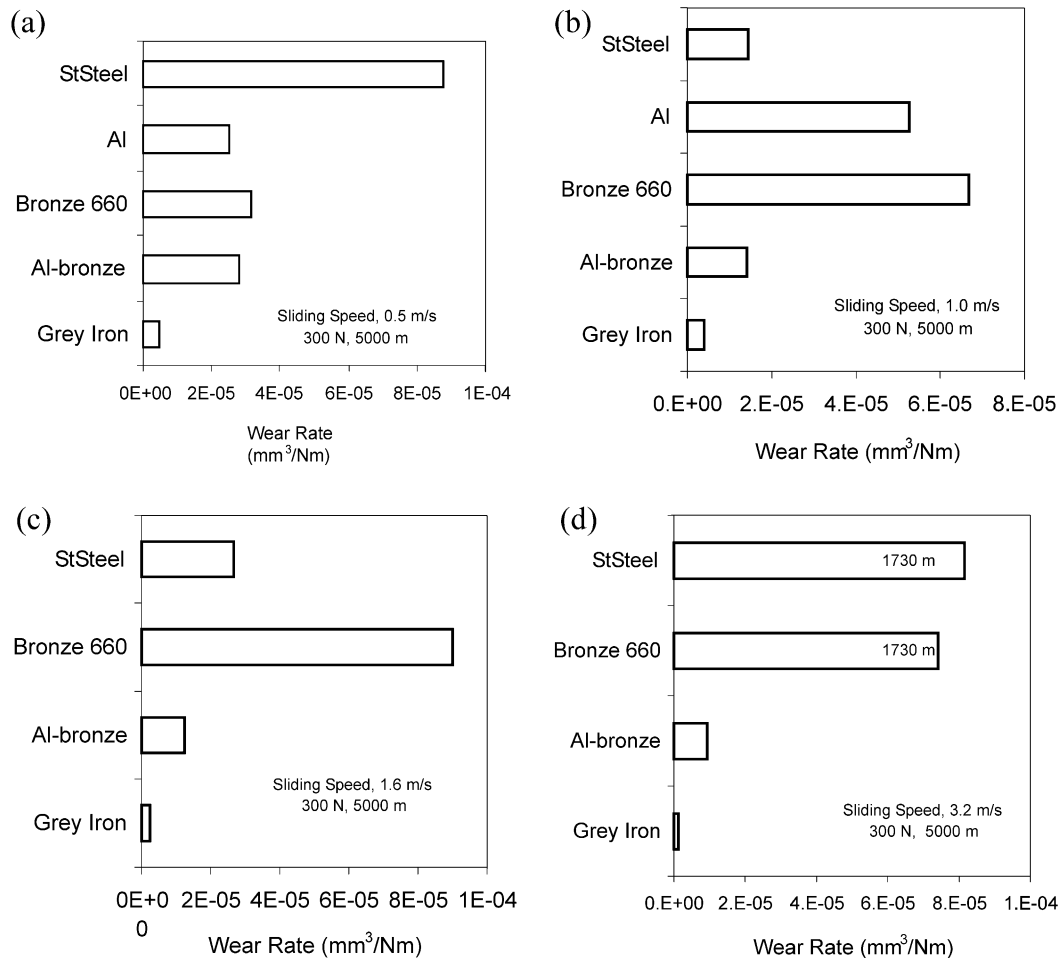


Fig. 12. Wear rate of various discs in sliding contact against  $\text{Si}_3\text{N}_4$  for different sliding speeds, (a) 0.5 m/s, (b) 1.0 m/s, (c) 1.6 m/s, (d) 3.2 m/s.

seen grey cast iron and Al-bronze resisted sliding wear fairly considerably at all times whereas stainless steel experienced high wear at both low and high sliding speeds. Although stainless steel exhibited good wear resistance at moderate speeds it proved a difficult mate in contact with silicon nitride due to high temperatures and noise levels generated. Bronze 660 and aluminium performed expectedly poor at all speeds.

## 5. Conclusions

The experimental findings on various materials in contact with silicon nitride under mineral oil lubricated sliding conditions at loads ranging from 16 to 300 N and at speeds changing from 0.5 to 4.0 m/s are summarised in the followings:

(1) The behaviour of grey cast iron and Al-bronze in sliding contact with silicon was characterised by a decrease in wear with an increase in sliding speed. Microscopic examinations revealed that the worn surfaces became smoother and smaller at higher sliding

speeds. Sliding caused relatively moderate temperature increases in the contact zone.

(2) High-lead-tin bronze (bronze 660) and aluminium experienced very high wear rates as sliding speed increased. The rise in the wear track temperature became significantly steeper with speed. A metallic tribofilm formation was visible at even very low speeds and low loads.

(3) Stainless steel experienced high wear and also caused significant damage to silicon nitride. A metallic tribofilm formed on the ceramic ball surface even at low speeds. Severity of wear between stainless steel and silicon nitride increased with the speed. High wear occurred at both low and high sliding speeds, which were accompanied by high wear track temperatures. This phenomenon resulted in considerable wear on both mating surfaces.

## References

- [1] G.W. Stachowiak, et al., Metallic film transfer during metal–ceramic unlubricated sliding, *Wear* 132 (1989) 361–381.

- [2] S. Lo Casto, et al., Wear mechanism of ceramic tools, *Wear* 160 (1993) 227–235.
- [3] S. Sasaki, The effects of surrounding atmosphere in friction and wear, in: K.C. Ludema (Ed.), *Proc. Int. Conf. on Wear of Materials*, ASME, 1989, pp. 409–417.
- [4] R.S. Gates, S.M. Hsu, Effect of selected chemical compounds on the lubrication of silicon nitride, *Tribol. Trans.* 34 (1991) 417–425.
- [5] A.J. Winn, et al., The lubricated wear of ceramics, *Tribol. Int.* 28 (5) (1995) 383–393.
- [6] X. Zhao, et al., Effect of antiwear additives on the friction and wear of  $\text{Si}_3\text{N}_4$  sliding contacts, *Wear* 201 (1996) 99–105.
- [7] J. Aucote, S.R. Foster, Use of ceramic tools when machining nickel base aerospace alloys, *Mater. Sci. Technol.* 2 (1986) 700–708.
- [8] S.K. Samanta, et al., Method of Using  $\text{Si}_3\text{N}_4$  System for Machining Cast Iron, US Patent 4,323,325, 6 April, 1982.
- [9] J. Vleugels, et al., Chemical interaction between a sialon cutting tool and iron based alloys, *Mater. Sci. Eng. A* 187 (1984) 177–182.
- [10] A. Skopp, et al., Tribological behaviour of silicon nitride materials under unlubricated sliding between 22 °C and 1000 °C, *Wear* 181–183 (1995) 571–580.
- [11] C. Melandri, et al., High temperature friction and wear testing of silicon nitride ceramics, *Tribol. Int.* 28 (6) (1995) 403–413.
- [12] P. Anderson, K. Holmberg, Limitation on the use of ceramics in unlubricated sliding applications due to transfer layer formation, *Wear* 175 (1994) 1–8.
- [13] L. Zhou, et al., Unlubricated sliding wear mechanism of fine ceramic  $\text{Si}_3\text{N}_4$  against high chromium cast iron, *Tribol. Int.* 27 (5) (1989) 349–357.
- [14] Y-Min. Gao, et al., An investigation on component and formation of tribochemical film in  $\text{Si}_3\text{N}_4$ /white iron sliding pair lubricated with distilled water, *Tribol. Int.* 30 (9) (1987) 693–700.